ISSN 1672-9145 **Acta Biochimica et Biophysica Sinica** 2005, **37**(8): 567–572 **CN** 31-1940/Q

Short Communication

Sequence-specific Assignment of ^{1}H-NMR Resonance and Determination of the Secondary Structure of Jingzhaotoxin-I

Xiong-Zhi ZENG, Qi ZHU, and Song-Ping LIANG*

College of Life Sciences, Hunan Normal University, Changsha 410081, China

Abstract Jingzhaotoxin-I (JZTX-I) purified from the venom of the spider *Chilobrachys jingzhao* is a novel neurotoxin preferentially inhibiting cardiac sodium channel inactivation by binding to receptor site 3. The structure of this toxin in aqueous solution was investigated using 2-D ^{1}H-NMR techniques. The complete sequence-specific assignments of proton resonance in the ^{1}H-NMR spectra of JZTX-I were obtained by analyzing a series of 2-D spectra, including DQF-COSY, TOCSY and NOESY spectra, in H_2O and D_2O. All the backbone protons except for Gln4 and more than 95% of the side-chain protons were identified by $d_{\alpha N}$, $d_{\alpha\delta}$, $d_{\beta N}$ and d_{NN} connectivities in the NOESY spectrum. These studies provide a basis for the further determination of the solution conformation of JZTX-I. Furthermore, the secondary structure of JZTX-I was identified from NMR data. It consists mainly of a short triple-stranded antiparallel β-sheet with Trp7-Cys9, Phe20-Lys23 and Leu28-Trp31. The characteristics of the secondary structure of JZTX-I are similar to those of huwentoxin-I (HWTX-I) and hainantoxin-IV (HNTX-IV), whose structures in solution have previously been reported.

Key words Jingzhaotoxin-I (JZTX-I); 2-D nuclear magnetic resonance (NMR); sequence-specific assignment; secondary structure

Spiders are remarkable for their reliance on predation as a trophic strategy. Their evolutionary success is largely a result of the production of a complex venom that is designed to quickly subdue or kill their prey [1]. Spider venom glands are extraordinary special organs that have evolved through hundreds of millions of years, and their secreted toxin components have special structural diversities and great specificity in terms of biological activities [2,3]. Many spider toxins have been used as invaluable tools for studying receptors, ion channels, nerve cell communication and immunology, and as potential lead structures in the design and creation of new highly specific and effective insecticides and pharmaceuticals [4,5]. Furthermore, antibodies raised against the critical toxin components have the potential to block the toxic effects and reduce the pain caused by spider envenomation [6].

Recently, a new peptide neurotoxin, Jingzhaotoxin-I (JZTX-I), purified from the venom of the spider *Chilobrachys jingzhao*, has been identified [7]. JZTX-I is a 33-residue peptide toxin containing three disulfide bridges Cys2-Cys17, Cys9-Cys22 and Cys16-Cys29, determined by partial reduction, sequencing and multi-enzymatic digestion. Moreover, JZTX-I is also an α-like sodium channel toxin first reported in spider venoms, inhibiting channel fast-inactivation kinetics of both TTX-resistant (TTX-R) voltage-gated sodium channels (VGSCs) on rat cardiac myocytes and TTX-sensitive (TTX-S) VGSCs expressed on rat dorsal root ganglion (DRG) neurons as well as cotton bollworm central nerve ganglia. It may contain important ligands for distinguishing cardiac VGSC subtypes [8].

In order to study the structure-function relationship of JZTX-I, we determined the structure of JZTX-I in solution using two-dimensional proton nuclear magnetic resonance (2-D ^{1}H-NMR) spectroscopy. The complete sequence-

Received: January 14, 2005 Accepted: May 9, 2005

This work was supported by grants from the National Natural Science Foundation of China (No. 30170193 and No. 30430170)

*Corresponding author: Tel, 86-731-8872556; Fax, 86-21-8861304; E-mail, liangsp@hunnu.edu.cn

DOI: 10.1111/j.1745-7270.2005.00078.x

specific assignments of proton resonances and the secondary structure of JZTX-I are reported in this paper.

Experimental Procedures

JZTX-I was isolated from the venom of the spider *Chilobrachys jingzhao* and purified by ion exchange and reverse phase high performance liquid chromatography (RP-HPLC) as described previously [8]. The purity of the peptide was confirmed by N-terminal sequencing, RP-HPLC and mass spectrometry analysis. The sample was prepared by dissolving the lyophilized powder of JZTX-I in 550 μl of buffer (H_2O:D_2O=9:1, *V*/*V*) containing 0.02% NaN_3 and 0.1 mM EDTA, with the final concentration of JZTX-I being 3.5 mM at pH 5.0. Sodium 3-(trimethylsilyl)propionate-2,2,3,3-D4 (TSP) was added to the mixture at a final concentration of 200 μM as an internal chemical shift reference. For experiments in D_2O, the sample used in H_2O experiments was lyophilized, redissolved in 99.8% D_2O, and then allowed to stand at room temperature for 24 h. After lyophilization, the peptide powder was redissolved in 550 μl of 99.96% D_2O (Cambridge Isotope Laboratories) [9].

The NMR spectra were collected on a Varian Inova 600 (Varian Inc, California, America) or a Bruker DRX-500 (Bruker BioSpin Corporation, Switzerland) spectrometer with a sample temperature of 300 K and 310 K, respectively. Two-dimensional DQF-COSY, TOCSY and NOESY measurements were recorded in a phase-sensitive mode by the time-proportional phase incrementation (TPPI) method following standard pulse sequences and phase cycling. TOCSY spectra were obtained with a mixing time of 85 ms and 100 ms. NOESY spectra were recorded in D_2O with a mixing time of 200 ms and in H_2O with a mixing time of 100 ms, 200 ms and 400 ms. Solvent suppression was achieved by the presaturation method. All 2-D measurements were recorded with 1024×512 frequency data points and were zero-filled to yield 2048×1024 data matrices except for the DQF-COSY spectrum. The DQF-COSY spectrum was recorded with 2048×512 data points in two dimensions, respectively, and zero-filled to yield 4096×1024 points to measure the coupling constants. All spectra were processed and analyzed using Felix 98.0 software (Biosym Technologies) running on a Silicon Graphics O2 workstation. The signal was multiplied by a sine bell square window function with a 90° phase shift in both dimensions prior to Fourier transformation.

As for the experiment involving the slow exchange of backbone amide protons, the sample lyophilized from H_2O was redissolved in D_2O and was identified by analyzing a series of 1-D spectra recorded at time points of 8 min, 15 min, 30 min, 1 h, 2 h, 3 h, 4 h, 5 h, 6 h and 24 h. A TOCSY spectrum was recorded after 6 h of exchange.

Results and Discussion

The sequence-specific proton resonance assignment of JZTX-I was performed using standard 2-D homonuclear NMR experiments [10]. It was performed in two steps: (1) identification of the spin systems; and (2) sequential assignment of resonances.

The 33 residues of JZTX-I were divided into four groups according to their spin systems and structural characteristics: (1) four Gly containing AX spin systems, each has two α protons; (2) seven residues containing methyl, including Ala1, Ala18, Ala21, Leu26, Leu28, Ile24 and Ile30; (3) fourteen AMX spin systems, including six Cys, three Trp, two Phe, Ser32, Asn19 and Tyr27; and (4) eight residues containing long side-chain spin systems, including three Lys, three Pro, Glu11 and Gln4. The proton resonances of JZTX-I were assigned to the spin systems of specific residue types by analyzing scalar coupling patterns observed in TOCSY and DQF-COSY spectra. The residue types that were immediately identified were Gly, Ala, Lys, Leu and Ile.

On the basis of the amino acid sequence of JZTX-I, 33 NH_i-$C_\alpha H_i$ cross-peaks were expected in the fingerprint region of the DQF-COSY spectrum because Ala1, Pro14, Pro15 and Pro33 do not exhibit cross-peaks, while four Gly exhibit eight cross-peaks. **Fig. 1** shows 26 NH_i-$C_\alpha H_i$ cross-peaks. Among them, the cross-peaks of Cys2, Gln4,

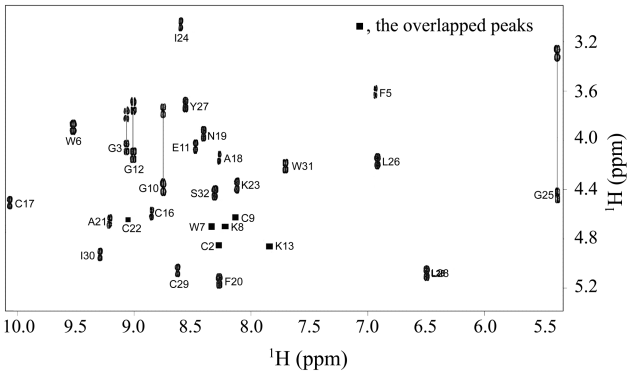

Fig. 1 Fingerprint region of the DQF-COSY spectrum of JZTX-I in H_2O

The NH_i-$C_\alpha H_i$ cross-peaks are shown.

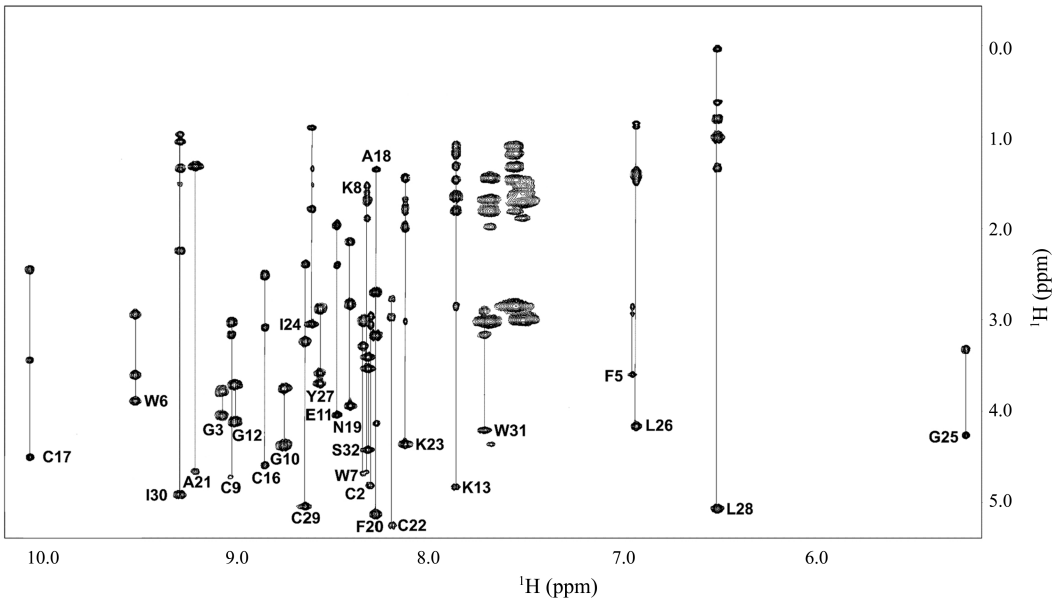

Fig. 2 Fingerprint region of the TOCSY spectrum of JZTX-I with a mixing time of 85 ms in H_2O at pH 5.0 and 300 K

All the spin systems of JZTX-I except for Ala1, Gln4, Pro14, Pro15 and Pro33 are shown.

Trp7, Lys8, Cys9, Lys13 and Cys22, can not be found. These peaks, except for Gln4, were overlapped by H_2O, but they were observed in NOESY and TOCSY spectra in D_2O. In the TOCSY spectrum with a mixing time of 85 ms, all the spin systems of JZTX-I, except for Ala1, Gln4, Pro14, Pro15 and Pro33, are shown in **Fig. 2**.

Sequence-specific assignments were carried out by looking for $d_{\alpha N}$, $d_{\beta N}$, $d_{\alpha\delta}$ and d_{NN} connectivities in the NOESY spectrum with a mixing time of 200 ms. Residue types that were previously assigned were used as starting points for the sequential assignment process. When a $d_{\alpha N}$-type NOE was observed, a sequential connectivity was established only if an additional $d_{\beta N}$ or d_{NN} NOE was also observed. The spin systems of residues Pro14, Pro15 and Pro33 were identified by the observation of strong sequential NOE cross-peaks between the α proton of the residue prior to the proline and the δ protons of the proline, which also indicate that residues Pro14, Pro15 and Pro33 in JZTX-I all take the *trans* configuration. Gly3, Gln4, Phe5, Lys8, Cys9, Cys22 and Lys23 were confirmed by the observed $d_{\beta N}$ and d_{NN} connectivities, although no sequential $d_{\alpha N(i,i+1)}$ connectivities were found. At the end of the sequential assignment procedure, all the backbone protons (except for Gln4) and more than 95% of the side-chain protons had been assigned. Although no NH-C_αH and NH-C_βH proton resonances of Gln4 were observed over the pH range of 4.0–6.5 and temperature range of 288–310 K, this complete lack of signals is possibly indicative of a chemical exchange which resulted in the undetectable ^{1}H resonances. **Fig. 3** shows the sequential $d_{\alpha N(i,i+1)}$ connectivities in the NH-C_αH fingerprint region of the NOESY spectrum with a mixing time of 200 ms. **Table 1** shows the summary of the chemical shifts of proton resonances of JZTX-I. All the amide protons of JZTX-I resonate at conventional frequencies with the exception of Gly25, which shows an unusual chemical shift for its amide proton (5.376 ppm at 300 K). During the structural calculations for JZTX-I, an explanation of this unusual chemical shift was obtained, when the Gly25 amide pro-

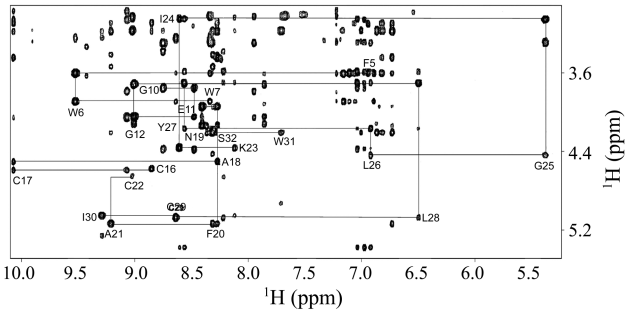

Fig. 3 Sequential $d_{\alpha N(i,i+1)}$ connectivities in the NH-C_αH fingerprint region of the NOESY spectrum with a mixing time of 200 ms in H_2O at pH 5.0 and 300 K

Sequential $d_{\alpha N}$ connectivity data are shown for residues 1-2, 5-7, 8-9, 10-13, 16-22 and 23-32.

Table 1 Chemical shifts of the assigned ^{1}H-NMR resonances of JZTX-I

Residue	NH	$C_\alpha H$	$C_\beta H$	Others
A1	–	4.177	1.630	–
C2	8.298	4.819	3.049, 2.966	–
G3	9.072	4.056, 3.787	–	–
Q4	–	4.667	3.095, 0.270	$C_\gamma H_2$ 1.759,1.524; $N_\delta H_2$ 7.249, 6.742
F5	6.938	3.600	2.931, 2.861	$C_{2,6}H$ 7.108; $C_{3,5}H$ 7.331; C_4H 7.164
W6	9.523	3.893	3.611, 2.943	C_2H 6.894; C_4H 7.052; C_5H 7.158; C_6H 7.208; C_7H 7.401; N_1H 9.696
W7	8.337	4.690	3.295, 3.013	C_2H 7.222; C_4H 7.949; C_5H 7.143; C_6H 7.284; C_7H 7.515; N_1H 10.318
K8	8.318	4.667	1.887, 1.700	$C_\gamma H_2$ 1.618, 1.536; $C_\delta H_2$ 1.712; $C_\varepsilon H_2$ 3.012
C9	8.219	4.658	3.377, 3.295	–
G10	8.749	4.385, 3.752	–	–
E11	8.477	4.045	1.970	$C_\gamma H_2$ 2.404
G12	9.007	4.127, 3.717	–	–
K13	7.858	4.831	1.806, 1.653	$C_\gamma H_2$ 1.184, 1.102; $C_\delta H_2$ 1.477, 1.325; $C_\varepsilon H_2$ 2.861
P14	–	4.681	2.451, 1.759	$C_\gamma H_2$ 2.240, 1.982; $C_\delta H_2$ 3.913, 3.611
P15	–	4.587	2.368, 2.052	$C_\gamma H_2$ 1.946, 2.052; $C_\delta H_2$ 3.705, 3.752
C16	8.849	4.596	3.084, 2.509	–
C17	10.071	4.514	3.447, 2.451	–
A18	8.272	4.139	1.360	–
N19	8.406	3.951	2.826, 2.146	–
F20	8.275	5.135	3.177, 2.697	$C_{2,6}H$ 6.730; $C_{3,5}H$ 6.821; C_4H 7.064
A21	9.212	4.667	1.325	–
C22	9.025	4.658	3.166, 3.037	–
K23	8.122	4.373	1.985, 1.782	$C_\gamma H_2$ 1.688,1.454; $C_\delta H_2$1.806; $C_\varepsilon H_2$ 3.025
I24	8.603	3.049	1.794	$C_\gamma H_2$ 1.524,1.348; $C_\gamma H_3$ 0.903
G25	5.376	4.455, 3.295	–	–
L26	6.920	4.162	1.430, 1.395	$C_\gamma H$ 1.489; $C_\delta H_3$ 0.891, 0.856
Y27	8.565	3.705	3.589, 2.884	$C_{2,6}H$ 7.042; $C_{3,5}H$ 6.986
L28	6.498	5.065	1.008, 0.797	$C_\gamma H$ 1.337; $C_\delta H_3$ 0.622, 0.035
C29	8.638	5.053	3.236, 2.392	–
I30	9.292	4.913	2.251	$C_\gamma H_2$ 1.523, 1.348; $C_\gamma H_3$ 1.055; $C_\delta H_3$ 0.973
W31	7.706	4.209	3.166, 2.908	C_2H 7.000; C_4H 7.278; C_5H 6.868; C_6H 6.800; C_7H 7.328; N_1H 9.907
S32	8.313	4.432	3.541, 3.412	–
P33	–	4.036	1.853	$C_\gamma H_2$ 1.785,1.633; $C_\delta H_2$ 3.283, 2.556

Data were obtained at pH 5.0, 300 K, TSP as referenced internal standard. Chemical shifts were measured to ±0.001 ppm.

ton was placed in the neighborhood of the aromatic ring of Tyr27. The ring current of Tyr27 creates an electromagnetic shield that dramatically affects the chemical shifts of the Gly25 amide proton. This was also observed for the chemical shifts of Gln4, which is similarly affected by the ring current of Trp7.

The regular secondary structure elements of the JZTX-I molecule were characterized according to the criteria described by Wüthrich [10]. The extent and relative orientation of β-strands were based on strong sequential $d_{\alpha N}$, interstrand d_{NN} and NH-$C_\alpha H$ connectivities, slow-exchange amide protons, and large $^3J_{NH\text{-}C_\alpha H}$ coupling constants, which distinguished the periphery and strands in the β-sheet. The NMR data summarized in **Fig. 4** show

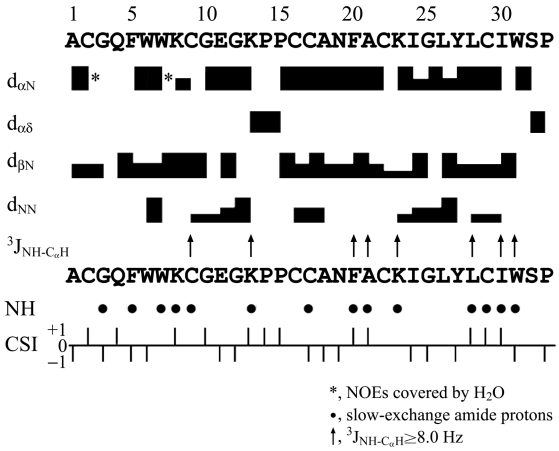

Fig. 4 Summary of the sequence NOE connectivities, $^3J_{NH\text{-}C_\alpha H}$ coupling constants and slow-exchange backbone amide protons observed in JZTX-I

Differences in NOE intensities (strong, medium, or weak) of the sequential $d_{\alpha N}$, $d_{\beta N}$, $d_{\alpha\delta}$ and d_{NN} connectivities are represented by the height of the bars. In the chemical shift index (CSI), plus and minus signs represent +1 and –1, respectively.

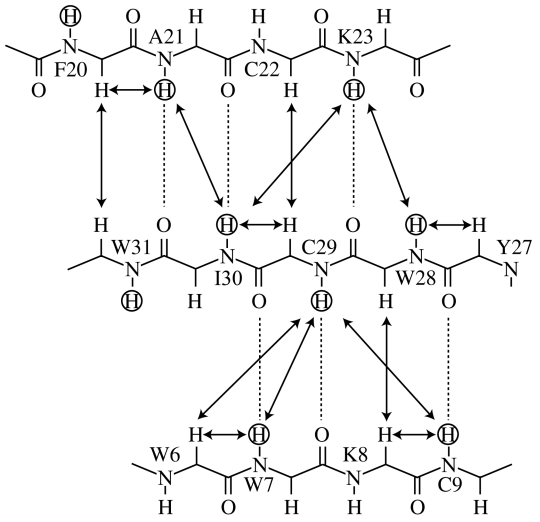

Fig. 5 Triple-stranded antiparallel β-sheet region (residues 7–9, 20–23 and 28–31) in JZTX-I

Observed NOEs are shown with arrows. Interstrand hydrogen bonds are shown with broken lines. Amide protons engaged in a slow exchange with heavy water are circled.

that there are three short β-strands from Trp7 to Cys9, Phe20 to Lys23, and Leu28 to Trp31. They are arranged in an antiparallel fashion with coils and turns. The analysis of the $C_\alpha H$ chemical shifts was in accordance with the three-strand antiparallel β-sheet, in which most of the residues showed downfield shifts [11]. **Fig. 5** shows the β-sheet region, which is in agreement with the standard criteria.

According to up-to-date records from the protein data bank, the 3-D solution structures of 32 spider toxins have been determined by using ^{1}H-NMR spectroscopy. Some of these toxins include the P-type calcium channel antagonist ω-agatoxin-IVA [12] and insect sodium channel inhibitor μ-agatoxins from the venom of the American funnel web spider [13]; the N-type calcium channel inhibitor HWTX-I [14], tetrodotoxin-sensitive sodium channel antagonist HWTX-IV [15] and SHL-I [16] from the Chinese bird spider *Selenocosmia huwena*; the potassium channel inhibitor Patx1 [17] from the venom of the spider *Phrixotrichus auratus*; the proton-gated cation channel blocker psalmotoxin 1 from the South American tarantula [18]; and the mechanosensitive ion channel inhibitor Gsmtx-4 [19] from the tarantula *Grammostola spatulata.* These toxins display low sequence homology and diverse bioactivity, but they all share the same structural scaffold known as the "inhibitor cystine knot" (ICK) architectural motif [20]. The ICK motif, which consists of several loops that emerge from a double-stranded or triple-stranded antiparallel β-sheet structure, is reticulated by at least three disulfide bridges. Two of the disulfide bridges, together with the amino acid backbone, form a ring, which is penetrated by the third disulfide bridge. However, the diverse bioactivities of those spider toxins derive from the local structural differences.

The structure of JZTX-I is characterized by a cystine knot and a small triple-stranded (Trp7 to Cys9, Phe20 to Lys23, and Leu28 to Trp31) antiparallel β-sheet. It is now evident that JZTX-I shares the same cystine knot motif as the spider toxins mentioned above on the basis of the secondary structure analysis.

In summary, the complete sequence-specific assignment of proton resonance in the ^{1}H-NMR spectra has been made and the secondary structure elements of JZTX-I have been obtained. These results will provide a basis for the structural calculation and detail analysis of JZTX-I.

Acknowledgements

We thank Mr. Xian-Zhong YAN of the National Center of Biomedical Analysis (China) and Guan-Zhong TU of the Beijing Institute of Microchemistry (Beijing, China) for collecting the ^{1}H-NMR spectra.

References

1 King GF. The wonderful world of spiders: Preface to the special toxicon issue on spider venoms. Toxicon 2004, 43: 471–475

2 Kordis D, Gubensek F. Adaptive evolution of animal toxin multigene families. Gene 2000, 261: 43–52

3 Rash LD, Hodgson WC. Pharmacology and biochemistry of spider venoms. Toxicon 2002, 40: 225–254

4 Escoubas P, Diochot S, Corzo G. Structure and pharmacology of spider venom neurotoxins. Biochimie 2000, 82: 893–907

5 Cestèle S, Catterall WA. Molecular mechanisms of neurotoxin action on voltage-gated sodium channels. Biochimie 2000, 82: 883–892

6 Zeng XZ, Xiao QB, Liang SP. Purification and characterization of raventoxin-I and raventoxin-III, two neurotoxic peptides from the venom of the spider *Macrothele raveni*. Toxicon 2003, 41: 651–656

7 Zhu MS, Song DX, Li TH. A new species of the family *theraphosidae*, with taxonomic study on the species *Selenocosmia hainana*. J Baoding Teachers College 2001, 14: 1–6

8 Xiao YC, Tang JZ, Hu WJ, Xie JY, Maertens C, Tytgat J, Liang SP. Jingzhaotoxin-I, a novel spider neurotoxin preferentially inhibiting cardiac sodium channel inactivation. J Biol Chem 2005, 280: 12069–12076

9 Li DL, Liang SP. Sequence-specific assignment of ^{1}H-NMR resonance and determination of the secondary structure of hainantoxin-I. Acta Biophysica Sinica 2003, 19: 359–365

10 Wüthrich K. NMR of Protein and Nucleic Acids. New York: Wiley 1986

11 Wishart DS, Sykes BD, Richards FM. The chemical shift index: A fast and simple method for the assignment of protein secondary structure through NMR spectroscopy. Biochemistry 1992, 31: 1647–1651

12 Kim JI, Konishi S, Iwai H, Kohno T, Gouda H, Shimada I, Sato K *et al*. Three-dimensional solution structure of the calcium channel antagonist ω-agatoxin IVA: Consensus molecular folding of calcium channel blockers. J Mol Biol 1995, 250: 659–671

13 Omecinsky DO, Holub KE, Adams ME, Reily MD. Three-dimensional structure analysis of mu-agatoxins: Further evidence for common motifs among neurotoxins with diverse ion channel specificities. Biochemistry 1996, 35: 2836–2844

14 Qu Y, Liang S, Ding J, Liu X, Zhang R, Gu X. Proton nuclear magnetic resonance studies on huwentoxin-I from the venom of the spider *Selenocosmia huwena*. 2. Three-dimensional structure in solution. J Protein Chem 1997, 16: 565–574

15 Peng K, Shu Q, Liu Z, Liang S. Function and solution structure of huwentoxin-IV, a potent neuronal tetrodotoxin (TTX)-sensitive sodium channel antagonist from Chinese bird spider *Selenocosmia huwena*. J Biol Chem 2002, 277: 47564–47571

16 Lu S, Liang S, Gu X. Three-dimensional structure of *Selenocosmia huwena* lectin-I (SHL-I) from the venom of the spider *Selenocosmia huwena* by 2D-NMR. J Protein Chem 1999, 18: 609–617

17 Chagot B, Escoubas P, Villegas E, Bernard C, Ferrat G, Corzo G, Lazdunski M *et al*. Solution structure of Phrixotoxin 1, a specific peptide inhibitor of Kv4 potassium channels from the venom of the theraphosid spider *Phrixotrichus auratus*. Protein Sci 2004, 13: 1197–1208

18 Escoubas P, Bernard C, Lambeau G, Lazdunski M, Darbon H. Recombinant production and solution structure of PcTx1, the specific peptide inhibitor of ASIC1a proton-gated cation channels. Protein Sci 2003, 12: 1332–1343

19 Oswald RE, Suchyna TM, McFeeters R, Gottlieb P, Sachs F. Solution structure of peptide toxins that block mechanosensitive ion channels. J Biol Chem 2002, 277: 34443–34450

20 Pallaghy PK, Nielsen KJ, Craik DJ, Norton RS. A common structural motif incorporating a cystine knot and a triple-stranded β-sheet in toxic and inhibitory polypeptides. Protein Sci 1994, 3: 1833–1839

Edited by
Hong-Yu HU